Equivalence between the nonlinear σ model and the spin-$\frac{1}{2}$ antiferromagnetic Heisenberg model: Spin correlations in La_2CuO_4

Efstratios Manousakis

Department of Physics, Center for Materials Research and Technology and Supercomputer Computations Research Institute,
Florida State University, Tallahassee, Florida 32306

Román Salvador

Control Data Corporation and Supercomputer Computations Research Institute, Florida State University,
Tallahassee, Florida 32306

We study the continuum limit of the quantum nonlinear σ model in 2+1 dimensions and at finite temperature T using both Monte Carlo simulation on large-size lattices ($100^2 \times 8$ is our largest-size lattice) and saddle-point approximation. At zero temperature, we find the critical point g_c that separates the quantum disordered phase from the phase with spontaneous symmetry breaking (nonzero staggered magnetization). We calculate the model's renormalization group β function close to the critical point. Using the β function, we rescale the correlation lengths calculated at various values of the coupling constant (spin stiffness) and temperature and find that they all collapse on the same curve $\xi/a_\sigma = f(T/T_\sigma)$. Even though the lattice spacing vanishes, a finite unit of length a_σ and a temperature scale T_σ is generated via *dimensional transmutation. Assuming* that the nonlinear σ model and the spin-$\frac{1}{2}$ antiferromagnetic (AF) Heisenberg model are equivalent at low temperature, we relate the units a_σ and T_σ to the lattice spacing a_H and the AF coupling J of the Heisenberg model so that the correlation lengths obtained from the simulation of the two models agree. In order to achieve this agreement we find that (a) the spin-$\frac{1}{2}$ AF Heisenberg model should order at $T=0$ and (b) the relationship between the scales a_σ, T_σ and a_H, J is obtained, and $f(T/T_\sigma)$ can be accurately approximated by an exponential of T_σ/T below g_c. We obtain a reasonable fit to the neutron scattering data of the insulator La_2CuO_4 by taking $J=1270$ K, a value close to that reported by Raman scattering experiments.

I. INTRODUCTION

It is the discovery of the copper-oxide superconductors[1] that intensified the study of certain theoretical models such as the antiferromagnetic (AF) Heisenberg model. The belief that the superconductivity mechanism in these materials is related to the strong correlations among purely electronic degrees of freedom[2] as well as neutron scattering experiments[3] which bring out strong two-dimensional spin correlations have given credit to the spin-$\frac{1}{2}$ AF Heisenberg model. Starting from one of the simplest models to take into account electron correlations in a nearly half-filled band such as the Hubbard model, the AF Heisenberg model can be obtained at half-filling by taking the strong-coupling limit.[4] In that formulation, the Heisenberg model

$$\hat{H} = J \sum_{\langle i,j \rangle} \mathbf{S}_i \cdot \mathbf{S}_j , \qquad (1.1)$$

describes interactions (that originate from virtual electron hopping processes) between the conduction-band electrons localized in the Wannier states around nearest-neighbor unit cells of the copper-oxide plane. Here $\mathbf{S}_i$ is the spin-$\frac{1}{2}$ operator of the ith cell.

Recently we simulated[5,6] the two-dimensional spin-$\frac{1}{2}$ AF Heisenberg model using Handscomb's quantum Monte Carlo method. We calculated the correlation length and we found that it increases very rapidly with decreasing temperature. Our results are consistent[6] with neutron scattering experiments. It is, however, difficult to find an efficient quantum Monte Carlo algorithm to study large systems and approach low temperatures.

It is believed[7] that the long-wavelength limit of the two-dimensional (2D) quantum Heisenberg model (1.1) is equivalent to the quantum nonlinear σ model in two-space one-Euclidean time dimensions. Namely, if a relationship between the parameters of the two models is appropriately established, the two models are equivalent in the parameter range where the correlation length is much larger than the lattice spacing. More recently there was a Soviet proposal[8] that in the derivation of the nonlinear σ model from the AF Heisenberg model one has to add a topological term in order to make the models equivalent. The consequences which such topological terms might have in the development of the theory of superconductivity in copper oxides, as well as the mathematical beauty which dresses such theories were part of the reason for the excitement about this direction of research. Later, however, the necessity of such topological terms became less clear, and in fact today the equivalence between the two models without any additional terms is still outstanding.[9]

The nonlinear σ model in 2+1 dimensions has recently

been studied by Chakravarty, Halperin, and Nelson (CHN).[10] Using one-loop perturbative renormalization-group approach, CHN relate the nonlinear σ model to the spin-$\frac{1}{2}$ AF Heisenberg model at low temperatures and give a good fit to the neutron scattering data[3] taken on La$_2$CuO$_4$.

Recently[11] we have simulated the nonlinear σ model in two-space one-Euclidean time dimensions and at finite physical temperature T using the Monte Carlo (MC) method. We found that we can make contact between the parameters of the spin-$\frac{1}{2}$ Heisenberg model and the nonlinear σ model by comparing the behavior of the correlation lengths at low temperatures. We also found good agreement with the results of the neutron scattering data[3] by taking $J = 1270$ K. The goal of the present paper is twofold. We offer more details about the simulation of Ref. 11 with new results obtained in the saddle-point approximation (SPA), and we also compare the results of the two different calculational schemes. In Sec. II of this paper we formulate the nonlinear σ model on the lattice, and in Secs. III and IV we describe the MC and SPA methods and compare them. In Sec. V we take the continuum limit of the nonlinear σ model in $2+1$ dimensions. We determine how the coupling constant of the theory (spin stiffness) should depend on the lattice spacing so that the results for the correlation length are independent of the cutoff. We calculate the model's renormalization-group β function around the three-dimensional critical point that separates the quantum disordered phase from the phase with spontaneous symmetry breaking (nonzero staggered magnetization). Using the β function we rescale the calculated correlation lengths at various couplings and temperatures and find that they all collapse on the same curve $\xi/a_\sigma = f(T/T_\sigma)$. Even though the lattice spacing vanishes, a finite unit of length a_σ and a temperature scale T_σ are generated via *dimensional transmutation*. In Sec. VI, the two parameters a_σ and T_σ of the σ model are related to the lattice spacing a_H and the AF coupling J of the Heisenberg model. The numerical relationship between a_σ, T_σ, and a_H, J is obtained by fitting $\xi(T) = f(T/T_\sigma)a_\sigma$ to the correlation length $\xi(T) = \xi_H(T/J)a_H$ obtained from the simulations of the spin-$\frac{1}{2}$ AF Heisenberg model. As a consequence of the *assumption* that the two models are equivalent at low T, we find that the spin-$\frac{1}{2}$ AF Heisenberg model must order at $T = 0$. We find that we need $J = 1270$ K to fit the neutron scattering data[3] for the spin-correlation length of the insulator La$_2$CuO$_4$.

II. FORMULATION

The nonlinear σ model in two-space one-Euclidean time dimensions is defined as[7,10]

$$S_{\text{eff}} = \frac{\rho_0}{2\hbar c} \int_0^{\beta\hbar c} d\tau \int dx\, dy [(\partial_x \Omega)^2 + (\partial_y \Omega)^2 + (\partial_\tau \Omega)^2] , \tag{2.1}$$

where Ω is a three-component vector field living on a unit sphere

$$\sum_{\alpha=1}^{n} \Omega_a^2 = 1 . \tag{2.2}$$

c is the bare (unrenormalized) spin-wave velocity, $\beta = (1/K_B T)$, and in the case of our interests $n = 3$. Transforming this problem on the $2+1$ dimensional lattice we obtain

$$S_{\text{eff}} = -\frac{1}{2g} \sum_{\mathbf{x}} \sum_{\mu=1}^{3} \Omega(\mathbf{x}) \cdot [\Omega(\mathbf{x} + \hat{e}_\mu) + \Omega(\mathbf{x} - \hat{e}_\mu)] , \tag{2.3}$$

where $\mathbf{x}$ covers the $2+1$ dimensional space-time lattice of lattice spacing a and size $N^2 N_\beta$, i.e., $x_1, x_2 = 1, 2, \ldots, N$, and $x_3 = 1, 2, \ldots, N_\beta$,

$$\beta\hbar c = N_\beta a , \tag{2.4}$$

and $g = \hbar c/\rho_0 a$. We have to impose a periodic boundary condition in the Euclidean time direction, i.e., $\Omega(\mathbf{x} + N_\beta \hat{e}_3) = \Omega(\mathbf{x})$. In this model, the average of the field Ω is proportional to the average staggered magnetization and could describe the dynamics of the spins within one isolated CuO$_2$ layer.

The generating functional $Z[J]$ defined as

$$Z[J] \equiv \int \prod_{\mathbf{x},\alpha} d\Omega_\alpha(\mathbf{x}) \exp\left[-S_{\text{eff}} + \sum_{\mathbf{x},\alpha} J_\alpha(\mathbf{x})\Omega_\alpha(\mathbf{x}) \right] \tag{2.5}$$

gives us the n-point correlation functions. For example, the two-point function is given by

$$G_{\alpha,\alpha'}(\mathbf{x},\mathbf{y}) = \frac{\int \prod_{\mathbf{x}',\alpha} d\Omega_\alpha(\mathbf{x}')\Omega_\alpha(\mathbf{x})\Omega_{\alpha'}(\mathbf{y})\exp(-S_{\text{eff}})}{\int \prod_{\mathbf{x}',\alpha} d\Omega_\alpha(\mathbf{x}')\exp(-S_{\text{eff}})} = \frac{1}{Z[J]} \frac{\delta^2 Z[J]}{\delta J_\alpha(\mathbf{x})\delta J_{\alpha'}(\mathbf{y})}\bigg|_{J=0} . \tag{2.6}$$

From the two-point function we can calculate the correlation length in lattice units ξ_{latt} as a function of g and for various values of N_β and N. We have to take the limit $N \to \infty$ and keep the time dimension finite so that Eq. (2.4) is satisfied. If, therefore, N is large enough so that

$$\xi_{\text{latt}} \ll N , \tag{2.7}$$

the correlation length is only a function of N_β and g, and in physical units is given by

$$\xi = \xi_{\text{latt}}(g, N_\beta)a . \tag{2.8}$$

For continuum limit behavior and for eliminating finite-size effects ξ_{latt} must satisfy

$$1 \ll \xi_{\text{latt}} \ll N . \tag{2.9}$$

III. MONTE CARLO SIMULATION

We used the heat-bath algorithm because in simulations of the classical $O(n)$ models[12] it seems superior over the Metropolis algorithm. In this method the field Ω at the site $\mathbf{x}$ is updated as follows. We calculate the sum over the fields at the neighboring sites,

$$\omega(\mathbf{x}) \equiv \sum_{\mu=1}^{3} \Omega(\mathbf{x}+\hat{e}_{\mu}) + \Omega(\mathbf{x}-\hat{e}_{\mu}) , \qquad (3.1)$$

and denote the polar and the azimuthal angles by θ and ϕ with respect to a local coordinate system having the z axis parallel to $\omega(\mathbf{x})$. The angle θ is drawn from the distribution

$$P(\theta) = \exp\left[\frac{1}{2g}\omega(\mathbf{x})\cos\theta\right] \qquad (3.2)$$

and the ϕ from a uniform distribution in the interval $(0, 2\pi)$. Finally we find the coordinates of $\Omega(\mathbf{x})$ with respect to a global coordinate system.

We extract the correlation length from the projected correlation function

$$G_p(\mathbf{r},\mathbf{r}') \equiv \langle \mathbf{s}(\mathbf{r})\cdot\mathbf{s}(\mathbf{r}') \rangle , \qquad (3.3a)$$

where

$$\mathbf{s}(\mathbf{r}) \equiv \frac{1}{N_\beta} \sum_{x_3=1}^{N_\beta} \Omega(\mathbf{x}) , \qquad (3.3b)$$

and $\mathbf{r}$ is only the space part of the vector $\mathbf{x}$. The average in Eq. (3.3a) is taken with respect to the distribution $e^{-S_{\text{eff}}}$. In our simulation we used periodic boundary conditions in the space boundaries also. Typically we used 5000 Monte Carlo steps over the entire lattice for
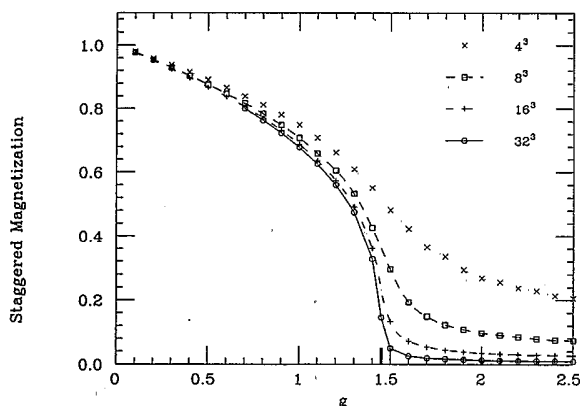

FIG. 1. The square root of the expectation value of the square of the average sigma field over the entire lattice in the nonlinear sigma model as a function of the coupling constant g. This corresponds to the staggered magnetization in the equivalent antiferromagnetic Heisenberg model. The calculation is performed at lattices of sizes 4^3, 8^3, 16^3, and 32^3. We also show the fixed point at $g_c = 1.45$ which we find and becomes the critical point at $T \rightarrow 0$ which correspond to the 3D critical point of the classical Heisenberg model.
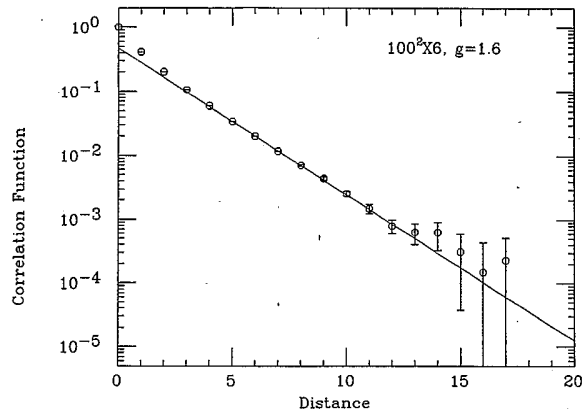

FIG. 2. The correlation function for lattice $100^2 \times 6$ and $g=1.6$. This value of g is above the 3D critical point $g_c=1.45$. Notice that on the logarithmic scale it drops as a straight line for several orders of magnitude up to the point where its value is as small as the error. The solid line is the result of the fit of the long distance behavior to the form given by Eq. (3.4).

thermalization and about 10 000 for measurements. In Fig. 1 the square root of the expectation value of the staggered magnetization squared (i.e., Ω^2) is plotted as a function of g for $N=N_\beta=4$, 8, 16, and 32. We see that the 3D critical point which is associated with spontaneous staggered magnetization is around $g=1.45$. In this paper we determine g_c accurately using finite-size scaling analysis.

In Fig. 2 we give the correlation function for $g=1.6$, $N=100$, and $N_\beta=6$. For periodic boundary conditions the correlation length is extracted by fitting the long-distance behavior of the correlation function with

$$G_p(x-x') = A(e^{-m_{\text{latt}}|x-x'|}$$
$$+ e^{-m_{\text{latt}}(N-|x-x'|)}) , \qquad (3.4)$$

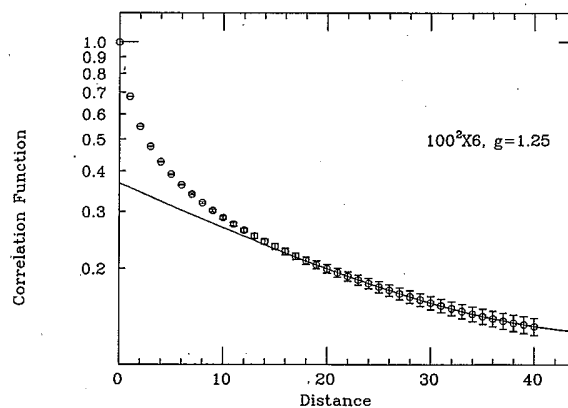i.e., with a $B \cosh[m_{\text{latt}}(N/2-|x-x'|)]$, where N is the

FIG. 3. A typical example of the correlation function below g_c. In this case the calculation is performed on a $100^2 \times 6$ lattice and $g=1.25$. The solid line is a fit of the large distance behavior of the correlation function to the form (3.4). See also Fig. 4.
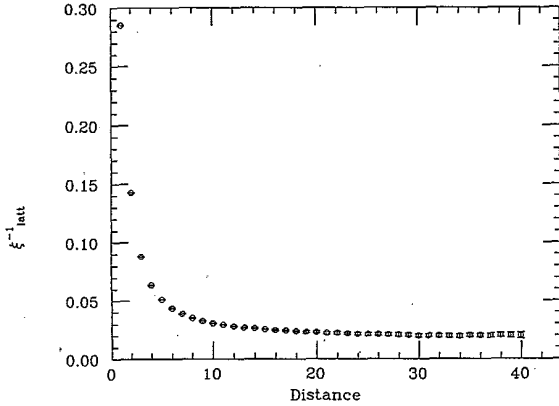
FIG. 4. The mass, i.e., the inverse correlation length as a function of the distance at which the correlation function is fitted to the form (3.4). We notice that the mass drops significantly over a distance of about 10 sites and stays constant for larger distances. This is the signature of the two different masses present in the theory for g smaller than the fixed point $g_c = 1.45$. For more details see text.

size of the one space direction. The solid line in Fig. 2 is the result of the fit. Notice that the correlation function on the logarithmic scale drops as a straight line by several orders of magnitude up to the point at which its value is as small as the error. The value of g in this case is above the critical point $g_c = 1.45$, namely, in the disorder phase where the n (n is the number of spin components and in our case $n=3$) modes of the theory have the same mass. In Fig. 3 we give a typical example of the correlation function below g_c for $g=1.25$ and the same size lattice. The two unknown parameters A and the mass $m_{latt} = \xi_{latt}^{-1}$ can be determined using only two neighboring points of the correlation function. In Fig. 4 we give the mass as a function of the distance of the first of these two points from the origin. We notice that the mass drops significantly over a distance of about 10 lattice sites and beyond that it stays constant. In the region $g < g_c$ there are two masses in the theory; namely, there are $n-1$ modes which correspond to the Goldstone-mode excitations and they become massless in the 3D theory ($\beta \rightarrow \infty$). They are related to the radial motion of the average field and they give an exponentially small mass with the size of the finite $\beta\hbar c$. There is also a massive mode associated with fluctuations in the magnitude (radial component) of the average field. Notice that even though the local field lives on a unit sphere and, therefore, does not have radial fluctuations, the average field over a large volume of the system can have fluctuating direction as well as magnitude. In this paper we study

the smallest mass, i.e., the larger correlation length which dominates the behavior of the correlation function at large distances [imagine that $G(r) = Ae^{-m_1 r} + Be^{-m_2 r}$ and because $m_1 > m_2$, $G(r) = Be^{-m_2 r}$ at large distances].

IV, SADDLE-POINT APPROXIMATION

The theory (2.3) with the field Ω satisfying the constraint (2.2) can be obtained from the following:

$$S_{eff} = \sum_x \left[-\frac{1}{2g} \sum_{\mu=1}^{3} \Omega(x) \cdot [\Omega(x+\hat{e}_\mu) + \Omega(x-\hat{e}_\mu)] + \lambda(\Omega^2(x)-1)^2 \right], \quad (4.1)$$

in the limit $\lambda \rightarrow \infty$. The additional term in that limit gives $\delta(\sum_{\alpha=1}^{n}\Omega_\alpha^2 - 1)$, which is the constraint (2.2). Hence, we can study the theory (4.1) and choose to take the limit $\lambda \rightarrow \infty$ at the end of the calculation. Using the identity

$$\sqrt{\alpha/\pi} \int d\rho(x)e^{-\alpha[\rho(x)-i\Omega^2(x)]^2} = 1, \quad (4.2)$$

we can introduce the auxiliary scalar field $\rho(x)$ in the generating functional $Z[J]$ on every site of the lattice. Using Eq. (4.1) for S_{eff} we can cancel the $\lambda(\Omega^2)^2$ by choosing $\alpha = \lambda$. Finally, shifting the field $\Omega(x)$ by a nonfluctuating vector field $C(x)$,

$$\Omega(x) = \phi(x) + C(x) \quad (4.3a)$$

and choosing $C(x)$ such that the coefficient of the term linear in $\phi(x)$ vanishes, i.e.,

$$\frac{1}{g} \sum_\mu [C(x+\hat{e}_\mu) + C(x-\hat{e}_\mu)] + 4\lambda[1+i\rho(x)]C(x) + J(x) = 0, \quad (4.3b)$$

we find

$$C(x) = g \sum_y K^{-1}(x,y)J(y). \quad (4.3c)$$

Here K^{-1} is the inverse of the matrix K which has matrix elements given by

$$K(x,y) = -\sum_{\mu=1}^{3} (\delta_{x,y+\hat{e}_\mu} + \delta_{x,y-\hat{e}_\mu} - 2\delta_{x,y}) - \delta_{x,y}\{6+4\lambda g[1+i\rho(x)]\}, \quad (4.3d)$$

and it is diagonal in the internal space of the components of the field. After some straightforward algebra we obtain

$$Z[J] = C' \int \prod_x d\rho(x) \prod_{x,\alpha} d\phi_\alpha(x) \exp\left[-\sum_x \left[\frac{1}{2g}\phi(x)\sum_y K(x,y)\phi(y) + \lambda\rho^2(x) \right] \right]$$

$$\times \exp\left[\frac{g}{2} \sum_{x,y,\alpha} J_\alpha(x)K^{-1}(x,y)J_\alpha(y) \right]. \quad (4.4)$$

The exponent of (4.4) is now quadratic in the ϕ field and hence it can be integrated out to obtain

$$Z[J] = C'' \int \prod_{\mathbf{x}} d\rho(\mathbf{x}) e^{-S'}$$

$$\times \exp\left[\frac{g}{2} \sum_{\mathbf{x},\mathbf{y},\alpha} J_\alpha(\mathbf{x}) K^{-1}(\mathbf{x},\mathbf{y}) J_\alpha(\mathbf{y})\right] , \tag{4.5}$$

and

$$S' = \lambda \sum_{\mathbf{x}} \rho^2(\mathbf{x}) + \frac{n}{2} \mathrm{Tr}[\ln(K)] . \tag{4.6}$$

We have, therefore, succeeded to eliminate the vector field Ω at the expense of another one-component field $\rho(\mathbf{x})$. The above expression can be the framework of a systematic expansion in $1/n$ for large n. Here we restrict ourselves to the saddle-point approximation which is the semiclassical approximation and also the zeroth order in a $1/n$ expansion. This is in very close analogy to the Wentzel-Kramers-Brillouin (WKB) semiclassical approximation which is also the leading order in an expansion in powers of $\hbar$. Several nontrivial phenomena may be understood in terms of the semiclassical approximation only.

From the saddle-point equation

$$\frac{\delta S'}{\delta \rho(\mathbf{x})} = 0 , \tag{4.7a}$$

for a translationally invariant solution [$\rho(x) = \mathrm{const}$], we obtain

$$\rho - ngi\frac{1}{V}\mathrm{Tr}(K^{-1}) = 0 , \tag{4.7b}$$

where

$$\mathrm{Tr}(K^{-1}) = \sum_{\mathbf{p}} \frac{1}{2\Sigma_\mu(1-\cos p_\mu) - \{6 + 4\lambda g[1+i\rho]\}} , \tag{4.7c}$$

where $p_\mu = n_\mu 2\pi/N_\mu$, $\mu = 1,2,3$, and $N_1 = N_2 = N$,

$N_3 = N_\beta$, and $n_\mu = 0,1,2,\ldots,N_\mu - 1$. The volume is $V = N^2 N_\beta$. We define

$$-m_0^2 \equiv 6 + 4\lambda g(1+i\rho) . \tag{4.8}$$

Then, m_0^2 is the solution of

$$\frac{1}{4n\lambda g^2}(m_0^2 + 4\lambda g + 6) = \frac{1}{V}\sum_{\mathbf{p}} \frac{1}{2\Sigma_\mu(1-\cos p_\mu) + m_0^2} . \tag{4.9}$$

The two-point correlation function (second derivative of $Z[J]$ with respect to J in the saddle-point approximation is given by $gK^{-1}(\mathbf{x},\mathbf{y})$ and in momentum space is given by

$$G(p) = \frac{g}{2\Sigma_\mu(1-\cos p_\mu) + m_0^2} . \tag{4.10}$$

To find the correlation length we transform the correlation function in Minkowski space and look for poles of the form $p_1 = p_2 = 0$, $p_3 = m$. The correlation length is given by $\xi_{\mathrm{latt}} = m^{-1}$ with m given as a solution of $2(1-\cosh m) + m_0^2 = 0$. We obtain

$$\xi_{\mathrm{latt}}^{\mathrm{SPA}} = \frac{1}{2\sinh^{-1}(m_0/2)} , \tag{4.11a}$$

and if $m_0 \ll 1$ then

$$\xi_{\mathrm{latt}} \simeq m_0^{-1} . \tag{4.11b}$$

Taking the limit $\lambda \to \infty$ we obtain

$$\frac{1}{ng} = \frac{1}{V}\sum_{\mathbf{p}} \frac{1}{2\Sigma_\mu(1-\cos p_\mu) + m_0^2} . \tag{4.12}$$

The above equation can be solved for m_0 numerically for any value of g and N_μ and find ξ_{latt} using (4.11). We will come back to the full solution of (4.12), but let us first give an approximate solution. Keeping N_β finite we take the limit $N \to \infty$ and after splitting off the zero mode ($p_3 = 0$) on the right-hand side, we obtain

$$\frac{1}{ng} = I_0 + I_1 , \tag{4.13a}$$

$$I_0 = \frac{1}{N_\beta}\int_{-\pi}^{\pi}\frac{d^2p}{(2\pi)^2}\frac{1}{2\Sigma_{\mu=1,2}(1-\cos p_\mu) + m_0^2} , \tag{4.13b}$$

$$I_1 = \frac{1}{N_\beta}\sum_{n_3=1}^{N_\beta}\int_{-\pi}^{\pi}\frac{d^2p}{(2\pi)^2}\frac{1}{2[1-\cos(2\pi n_3/N_\beta) + 2\Sigma_{\mu=1,2}(1-\cos p_\mu) + m_0^2]} . \tag{4.13c}$$

Let k be some small momentum cutoff, so that for $|p| < k$ we have

$$\Sigma_{\mu=1,2}\cos(p_\mu) \simeq 2 - p^2/2 .$$

We may write

$$I_0 \simeq \frac{2}{N_\beta}\int_0^k\frac{d^2p}{(2\pi)^2}\frac{1}{p^2 + m_0^2}$$

$$+ \frac{2}{N_\beta}\int_k^\pi\frac{d^2p}{(2\pi)^2}\frac{1}{2\Sigma_{\mu=1,2}(1-\cos p\mu) + m_0^2} . \tag{4.14}$$

Assuming that there is a range of g where $m_0 \rightarrow 0$ as $N_\beta \rightarrow \infty$, we obtain

$$I_0 \simeq -\frac{1}{2\pi N_\beta}\ln(m_0^2)+I_2 , \qquad (4.15a)$$

$$I_2 = \frac{1}{2\pi N_\beta}\ln(k^2+m_0^2)$$

$$+\frac{2}{N_\beta}\int_k^\pi \frac{d^2p}{(2\pi)^2}\frac{1}{2\Sigma_{\mu=1,2}(1-\cos p_\mu)+m_0^2} . \qquad (4.15b)$$

Therefore,

$$m_0^2 = e^{-2\pi f N_\beta} , \qquad (4.16a)$$

$$f = \frac{1}{ng}-(I_1+I_2) , \qquad (4.16b)$$

and in order to satisfy our assumption $m_0(N_\beta \rightarrow \infty)=0$, we must have

$$g < g_c , \qquad (4.17a)$$

$$g_c = \frac{1}{(I_1+I_2)n} . \qquad (4.17b)$$

Hence, the correlation length

$$\xi(T \rightarrow 0) = a \exp\left[\frac{\pi \hbar c f}{a K_B T}\right] \qquad (4.18)$$

in the SPA approximation for $g < g_c$.

Given values for N, N_β, and g we can solve Eq. (4.12) numerically for m_0 and obtain ξ_{latt}. In Fig. 5 we compare the MC data for $50^2 \times 4$ with the solution of the SPA Eq. (4.12) for the same parameter values and lattice size. We
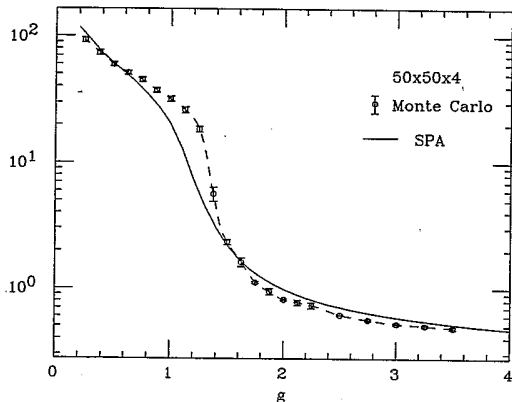

FIG. 5. Comparison of the correlation lengths as calculated from MC simulation and the SPA. Both calculations are performed at a finite lattice of size $50^2 \times 4$ to make the comparison meaningful. We note that they have similar overall qualitative behavior but they have significant quantitative differences. For small correlation lengths and in the region where we have strong-finite size effects ($\xi > 20$) MC and SPA agree. For correlation lengths in the region close to the fixed point which is the interesting region close to the fixed point which is the interesting region we notice significant disagreement.
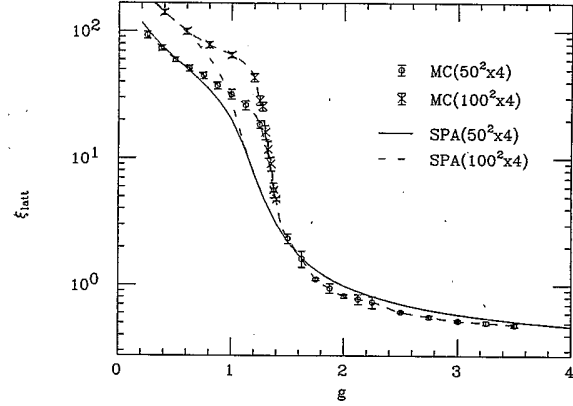

FIG. 6. Study of the finite-size effects. We plot the correlation lengths calculated for lattices of sizes $50^2 \times 4$ and $100^2 \times 4$ by both Monte Carlo and saddle-point approximation. We notice that both calculations feel finite-size effects for $\xi_{latt} > 20$.

note that the overall behavior is similar, but there are significant differences. For small correlation lengths and in the regions where we have strong finite-size effects the SPA and the MC results agree reasonably well. But for larger correlation lengths with small finite-size effects the results are very different. In Fig. 6 we give the correlation length obtained from the Monte Carlo calculation for lattices $50^2 \times 4$ and $100^2 \times 4$. We notice that the correlation lengths feel strong finite-size effects when $\xi_{latt} > 20$ which is somewhat smaller than half the size of the smaller lattice (because of the periodic boundary conditions). In the same figure we plotted the results of SPA for the same lattices. We see that the finite-size effects begin at correlation lengths of about the same size.

There are two directions to improve upon the saddle-point solution: (a) We can take into account small fluctuations around the saddle point by writing

$$\rho(\mathbf{x}) = \rho_0 + \chi(\mathbf{x}) \qquad (4.19)$$

and expand S' in powers of $\chi(\mathbf{x})$ and keep terms up to $\chi^2(\mathbf{x})$. The integrals in the fluctuating field $\chi(\mathbf{x})$ are Gaussian and they can be carried out explicitly. (b) There may be nontranslational invariant solutions to the saddle-point equation with nontrivial topological structure. It is not known, however, how to calculate the entropy of all possible classical nonconstant configurations.

In the rest of this paper, however, we would like to focus on our results obtained by means of a nonperturbative method such as the Monte Carlo simulation. We will only use the results of the SPA for comparison and as a guide.

V. CONTINUUM LIMIT OF THE NONLINEAR σ MODEL DIMENSIONAL TRANSMUTATION

First, let us keep the physical temperatuare constant. Using Eq. (2.4) we obtain

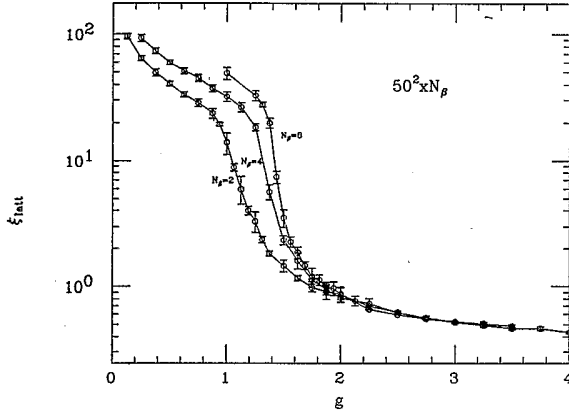$$a = \frac{\hbar c \beta}{N_\beta} . \qquad (5.1)$$

FIG. 7. The correlation lengths in lattice units calculated with Monte Carlo for lattice sizes $50^2 \times N_\beta$ with $N_\beta = 2, 4, 8$ as a function of g.

FIG. 9. The ratio $b = \xi_{\text{latt}}/N_\beta$, i.e., the correlation lengths in units of $a_T \equiv (\hbar c / K_B T)$ as calculated in the saddle-point approximation. Notice that all the lines for different N_β pass through the same point $(g_c, b^*) = (1.325 \pm 0.01, 0.98 \pm 0.05)$.

Increasing N_β we approach the continuum limit $(a \rightarrow 0)$ at constant temperature. To keep the correlation length ξ constant in physical units for any a, we should find the value of g which gives the same value of ξ. This is achieved through Eq. (2.8) which defines the function $g(a)$. In Fig. 7 we plot $\xi_{\text{latt}}(g, N_\beta)$ for lattice size $50^2 \times N_\beta$ where $N_\beta = 2, 4, 8$. The combination of Eq. (2.8) and Eq. (5.1) gives

$$\xi = \frac{\xi_{\text{latt}}(g, N_\beta)}{N_\beta} \frac{\hbar c}{K_B T} . \tag{5.2}$$

In order to keep ξ constant at a fixed temperature we should keep the ratio

$$b = \frac{\xi_{\text{latt}}(g, N_\beta)}{N_\beta} \tag{5.3}$$

constant. b is the physical value of the correlation length at temperature T in units of $a_T \equiv (\hbar c / K_B T)$. In Fig. 8
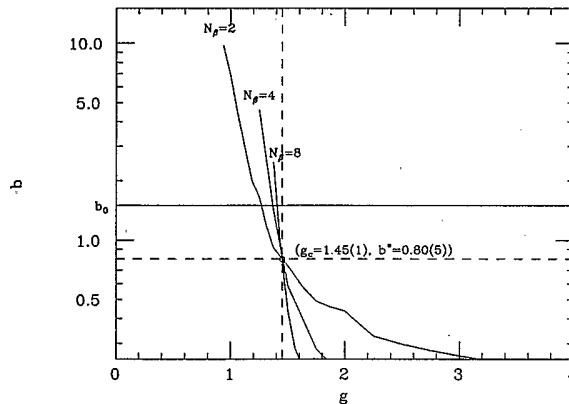
we give b as a function of g for several values of N_β. We notice that the lines for various N_β pass through the same point $(g_c, b^*) = (1.45 \pm 0.01, 0.80 \pm 0.05)$. Let us say that we would like to define the theory's coupling constant at the value $b = b_0$ shown in Fig. 8. The line $b = b_0$ intersects the various curves for different N_β's (i.e., in this case with constant temperature for different a's), and the value of g's at the intersections define $g(a_T / N_\beta)$. We note that

$$\lim_{N_\beta \rightarrow \infty} g(a_T / N_\beta) = g_c . \tag{5.4}$$

This value corresponds to the curve with infinite slope at $g = g_c$. Note that if we choose to define the theory at $b = b^*$ then $g(a_T / N_\beta) = g_c$ for large N_β, i.e., for small a. Because

$$b = \frac{\xi_{\text{latt}}(g, N_\beta)}{N_\beta} = b^*$$

at g_c, we obtain

FIG. 8. The ratio $b = \xi_{\text{latt}}/N_\beta$, i.e., the correlation lengths in units of $a_T \equiv (\hbar c / K_B T)$ as calculated by Monte Carlo simulation for lattices of sizes $50^2 \times N_\beta$ with $N_\beta = 2, 4, 8$. Notice that all the lines for different N_β pass through the same point $(g_c, b^*) = (1.45 \pm 0.01, 0.80 \pm 0.05)$. The solid line is obtained by joining the data points by straight lines.
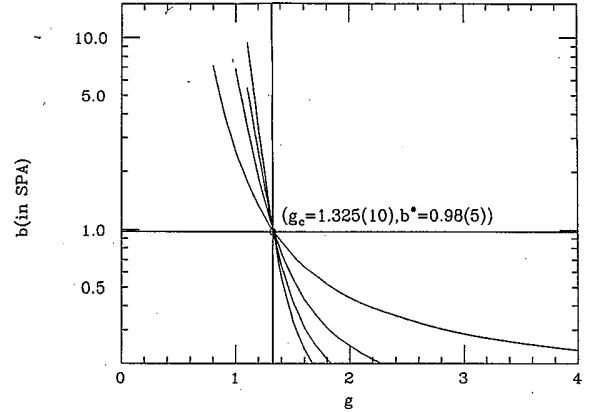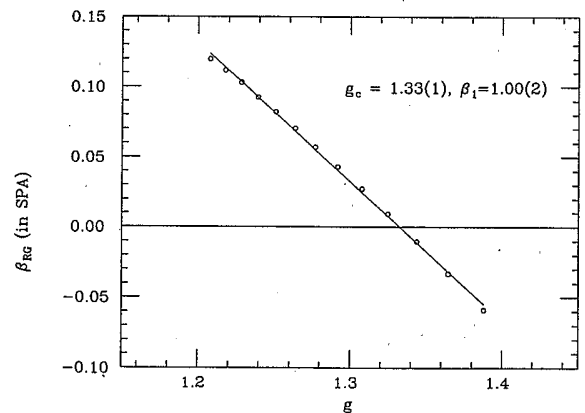

FIG. 10. The renormalization group β function calculated in the SPA around the fixed point. The values of the parameters depicted on the graph correspond to a linear fit to the form $\beta_{\text{RG}} = -\beta_1 (g - g_c)$.

$$\xi^* = b^* \frac{\hbar c}{K_B T} , \qquad (5.5)$$

where $b^* = 0.80 \pm 0.05$. Notice that at $T = 0$ this point turns into a critical point (this is the critical point of the 3D classical Heisenberg model). We have also performed calculations for lattices with sizes $100^2 \times N_\beta$ with various values of g. Table I lists the values of the correlation lengths obtained for $50^2 \times N_\beta$ and $100^2 \times N_\beta$ sized lattices with $N_\beta = 2, 4, 6, 8$ as a function of g.

In Fig. 9 we give b calculated in the SPA for $N_\beta = 2, 4, 6, 8$ and N large enough so that the data shown are free of finite-size effects. We notice the same behavior. In this

approximation $g_c = 1.325 \pm 0.010$, smaller than the MC value, and $b^* = 0.98 \pm 0.05$ which is bigger than the MC value.

The renormalization group (RG) β function,

$$\beta_{RG} \equiv -a \frac{dg(a)}{da} , \qquad (5.6)$$

can be calculated from the results of the SPA or MC calculation. The curves of Figs. 8 and 9 for $N_\beta = 2, 4, 6$, correspond to lattice spacings $a_T/2$, $a_T/4$, and $a_T/6$, respectively. At a fixed value of ξ we can find the intersections $g(a_T/N_\beta)$ and take the derivative (5.6). We can re-

TABLE I. The values of the correlation lengths $\xi_{latt}(g, N, N_\beta)$ in lattice spacing units as calculated from the Monte Carlo simulation of the nonlinear sigma model. The calculation was done on a $N^2 \times N_\beta$ with $N = 50$, $N_\beta = 2, 4, 8$ and $N = 100$, $N_\beta = 2\ 4, 6, 8$ and at several values of g.

g	$N=50$			$N=100$			
	$N_\beta=2$	$N_\beta=4$	$N_\beta=8$	$N_\beta=2$	$N_\beta=4$	$N_\beta=6$	$N_\beta=8$
0.125	96(5)						
0.25	65(3)	93(6)					
0.375	49(4)	74(4)					
0.5	41(2)	60(3)					
0.625	33(2)	51(3)					
0.75	29(2)	45(3)					
0.875	24(2)	37(3)					
0.9375	19.4(7)						
1	14(3)	32(3)	49(6)				
1.0625	8.8(7)						
1.125	6(2)	26(3)					
1.1875	4.0(4)						
1.25	3.3(6)	18(2)	33(3)	3.3(3)	29(3)	43(2)	
1.275				2.75(7)	26(2)	44(3)	
1.3				2.60(9)	16(2)	43(2)	
1.3125	2.4(2)		28(2)				
1.325				2.33(8)	12.0(7)	32(2)	
1.35				2.00(3)	9.1(8)	22(4)	
1.375	1.83(8)	5.7(8)	20(2)	1.92(2)	5.7(2)	14(2)	27(3)
1.4				1.77(3)	5.0(2)	10.2(9)	21(2)
1.4375			7.4(8)				
1.5	1.5(2)	2.3(2)	3.5(6)				
1.5625			2.3(2)				
1.625	1.16(6)	1.6(3)	1.9(2)				
1.6875			1.5(1)				
1.75	0.98(7)	1.12(3)	1.2(3)				
1.8125			1.1(2)				
1.875	0.9(2)	0.95(8)	0.99(9)				
1.9375			1.0(2)				
2	0.9(1)	0.82(3)	0.9(2)				
2.125		0.77(7)					
2.25	0.653(9)	0.73(8)	0.70(1)				
2.5	0.594(5)	0.61(1)	0.62(2)				
2.75	0.551(7)	0.56(2)					
3	0.52(1)	0.52(2)					
3.25	0.49(2)	0.51(2)					
3.5	0.47(1)	0.48(2)					
3.75	0.47(2)						
4	0.435(9)						

peat this for various ξ's. The results for β_{RG} obtained using the correlation lengths in the SPA behave as shown in Fig. 10. At $g = g_c$, β_{RG} changes sign. At $T = 0$, $\xi_c = \infty$, and for $g < g_c$ the system enters to a phase with spontaneous symmetry breaking, where the staggered magnetization is nonzero. We see that close to the critical point $\beta_{\text{RG}}(g)$ is clearly linear and

$$\beta_{\text{RG}}(g) = -\beta_1(g - g_c) + \cdots . \tag{5.7}$$

In the case of SPA, we find $g_c = 1.33 \pm 0.01$ and $\beta_1 = 1.00 \pm 0.02$.

In Fig. 11 we present the $\beta_{\text{RG}}(g)$ obtained from the MC calculation using correlation lengths up to $b = 2.5$. We see a similar linear behavior giving $g_c = 1.450 \pm 0.003$ and $\beta_1 = 1.28 \pm 0.05$.

We can integrate Eq. (5.6) to obtain $a(g)$

$$a = a_\sigma \exp\left[-\int^g \frac{dg}{\beta_{\text{RG}}(g)} \right] , \tag{5.8}$$

where a_σ is a constant of integration. The above equation defines the function $g(a)$ which characterizes the continuum theory. a_σ is a characteristic parameter of the theory and the cutoff should be removed in such a way that the combination

$$a_\sigma = a \exp\left[\int^g \frac{dg}{\beta_{\text{RG}}(g)} \right] \tag{5.9}$$

remains finite. In field theory, the phenomenon in which a vanishing length scale $(a \to 0)$ and a dimensionless parameter (g) produce a dimensional quantity (a_σ) with units of length is called *dimensional transmutation.*[13]

Using the linear approximation [Eq. (5.7)] close to the critical point we find

$$a(g) = a_\sigma |g - g_c|^{1/\beta_1} . \tag{5.10}$$

The constant a_σ is determined by the physical value we assign to the correlation length at given values of the oth-

er parameters. Namely, its value will be determined from the phenomena which this theory is assumed to describe. This operation is the goal of the next section of this paper.

Combining Eqs. (2.4) and (5.10) we obtain

$$N_\beta = |g - g_c|^{-1/\beta_1} \frac{T_\sigma}{T} , \tag{5.11a}$$

where

$$K_B T_\sigma = \frac{\hbar c}{a_\sigma} . \tag{5.11b}$$

Substituting $a(g)$ and N_β from Eqs. (5.10) and (5.11a) into Eq. (2.8) we obtain

$$\xi / a_0 = f\left[\frac{T}{T_\sigma} \right] , \tag{5.12a}$$

where we have defined f as follows:

$$f(T/T_\sigma) \equiv \xi_{\text{latt}}\left[g, |g - g_c|^{-1/\beta_1} \frac{T_\sigma}{T} \right] |g - g_c|^{1/\beta_1} . \tag{5.12b}$$

Since the constants a_σ and T_σ are independent of g and ξ is also independent of g in the process of removing the cutoff, the function in Eq. (5.12b) is only a function of the ratio $t \equiv T/T_\sigma$. In Fig. 12 we show the function $f(t)$. The data points in the figure are those of Table I with $\xi_{\text{latt}} < 25$ and they correspond to various $g < g_c$ and N_β values. We see that all scale to a universal curve. Again, we emphasize the occurrence of *dimensional transmutation* where, although the lattice spacing is removed together with g we obtain correlation lengths in units of a finite constant a_σ as a function of temperature t in units of T_σ.

The curve $f(t)$ can be approximated by an exponential

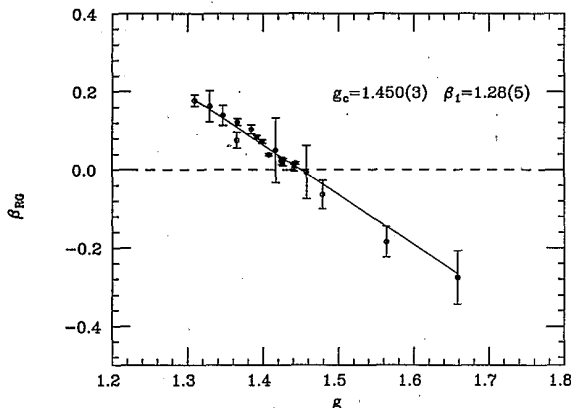$$f(t) = A_\sigma \exp(B_\sigma / t) . \tag{5.13}$$

FIG. 11. The renormalization group β function calculated using our Monte Carlo data around the fixed point. The values of the parameters depicted on the graph correspond to a linear fit to the form $\beta_{\text{RG}} = -\beta_1(g - g_c)$.
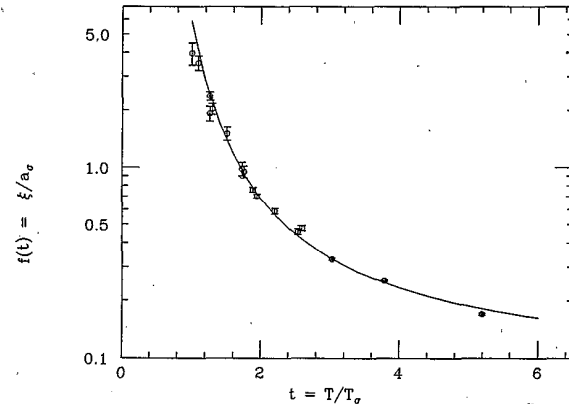

FIG. 12. The rescaled correlation lengths [i.e., the function $f(t)$, see text] in the σ model using the calculated renormalization group β function. Even though the lattice spacing vanishes, dimensional transmutation occurs giving rise to a finite unit of length a_σ and unit of temperature T_σ.
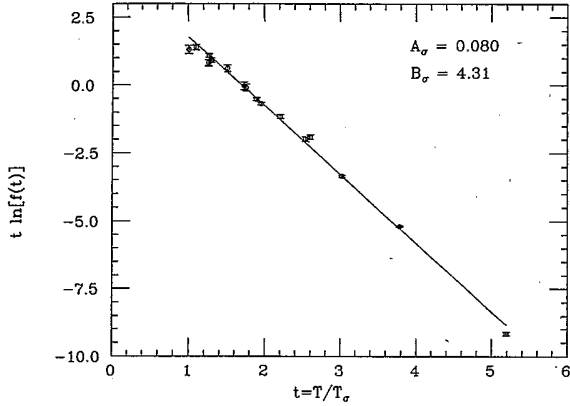
FIG. 13. A demonstration that the function $T/T_\sigma \ln[f(T/T_\sigma)]$ fits to a straight line.

To demonstrate this, in Fig. 13 we plot the function $t \ln[f(t)]$ and we see a straight line which intersects the y axis at $B_\sigma = 4.31$ and has a slope $\ln(A_\sigma) = -2.53$. In Fig. 12 the solid line corresponds to the exponential (5.13) with the above parameters. We would like to remind the reader that in SPA we also found an exponential form [Eq. (4.18)].

In the next section we shall attempt to make contact between this model, the spin-$\frac{1}{2}$ AF Heisenberg model and the experiment. To close the discussion about the nonlinear σ model, going back to Fig. 7, we may notice that $\xi_{\text{latt}}(g, N_\beta) = f(g)$ for $g \gg g_c$, i.e., a function independent of N_β. Hence, Eq. (2.8) yields that ξ is only a function of g,

$$\xi(g \gg g_c) = f(g)a(g) . \tag{5.14}$$

The function $\xi(g)$ is independent of T and therefore can be determined by performing the calculation at $T = 0$. Finally, for $g < g_c$, i.e., in the region which is characterized with order at $T = 0$ (where $\xi = \infty$), ξ is growing faster than $1/T$ with decreasing T. The SPA solution and our numerical data suggest an exponential increase with $\beta = 1/T$ [Eqs. (4.18) and (5.13)].

These results confirm the crossover phase diagram given by CHN.[10] In their more recent paper, they also use the exponential form for ξ with a constant prefactor. They also obtain the relation (5.5) and find $b^* = 1.1$ a value close to our SPA result but somewhat higher than our MC result.

VI. NONLINEAR σ MODEL, SPIN-$\frac{1}{2}$ HEISENBERG ANTIFERROMAGNETIC MODEL AND EXPERIMENT

We would like to discuss the possibility of making contact between the spin-$\frac{1}{2}$ AF Heisenberg model and the nonlinear σ model. In Refs. 5 and 6 we simulated the former and we found it to grow much more rapidly than $1/T$. More precisely, in Ref. 5, we fit the correlation lengths to two different forms:

$$\xi(T) = C/T e^{b/T} , \tag{6.1}$$

and

$$\xi(T) = C e^{b/|T-T_c|^{1/2}} , \tag{6.2}$$

and we found that the latter form fits better and concluded that our simulation indicated that topological excitations may play an important role in the dynamics of the spin-$\frac{1}{2}$ Heisenberg antiferromagnet. Following our findings for the σ model we attempt to fit our numerical results for the Heisenberg model to

$$\xi/a_H = A_H \exp(B_H J/T) . \tag{6.3}$$

This form, i.e., without the $1/T$ prefactor, fits our data equally well as the form (6.2), as shown in Fig. 14. The fit gives (see dashed line labeled $l = 0$ in Fig. 7 of Ref. 6) $A_H 0.25 \pm 0.01$ and $B_H = 1.4 \pm 0.05$ (see Table II of Ref. 6 and $B_H = 2\pi b$ in the notation of Ref. 6). In Fig. 14 we plot the function $T/J \ln(\xi/a_H)$ using the results of our calculation.[5,6] The intersection with the $T = 0$ axis gives B_H and the slope $\ln(A_H)$. The straight line fit gives $A_H = 0.25$ and $B_H = 1.43$. In the last section we saw that the nonlinear σ model has three different phases: (1) a phase with $g > g_c$, where the correlation length is a constant independent of T, (2) a critical point at $g = g_c$ where the correlation length is proportional to $1/T$, and (3) a phase with spontaneous staggered magnetization at $T = 0$ for $g < g_c$, where for finite T the correlation length grows approximately exponentially with $1/T$ as the temperature is lowered. Among the three forms the exponential fits better to the $\xi(T)$ of the spin-$\frac{1}{2}$ AF Heisenberg model. Furthermore, assuming that the two models are equivalent at low T we conclude that the spin-$\frac{1}{2}$ AF Heisenberg model should order at $T = 0$ and the results of our simulation[5,6] may also be consistent with spin-wave theory and existence of an ordered state at $T = 0$. Equivalence between the two models requires

$$A_H a_H = A_\sigma a_\sigma , \tag{6.4}$$

$$B_H J = B_\sigma T_\sigma . \tag{6.5}$$

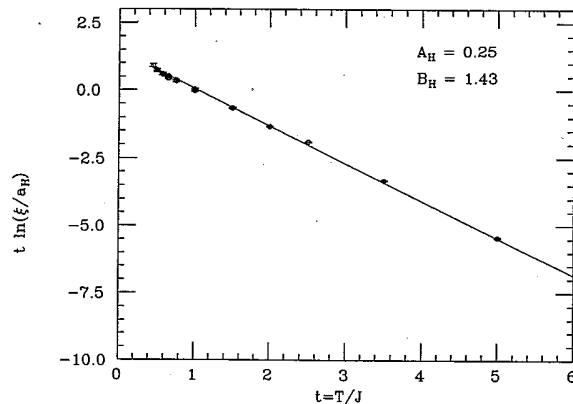From Eq. (6.4) we obtain $a_\sigma = 3.14 a_H$, from Eqs. (6.5)

FIG. 14. A demonstration that the function $T/J \ln[\xi_H(T/J)]$ fits to a straight line.

$T_\sigma = 0.325J$, from (5.11b) we obtain $\hbar c \simeq 1.04 Ja_H$. In Oguchi's calculation[14] for a spin-S antiferromagnet, the renormalized spin-wave velocity is

$$\hbar c_r = 2\sqrt{2}s(1 + 0.158/2s)Ja_H .$$

For a spin-$\frac{1}{2}$ antiferromagnet, its value $\hbar c_r = 1.64 Ja_H$, is lower than our value for the bare spin-wave velocity which enters in the nonlinear σ model. More recently Gomez-Santos, Joannopoulos, and Negele (GJN) (Ref. 15) have performed similar simulations of the spin-$\frac{1}{2}$ AF Heisenberg model. They find overall agreement with our results at higher temperatures reported in Ref. 5, but they find smaller correlation lengths at lower temperatures. GJN argue that the origin of the discrepancy may be that their new algorithm searches the phase space more efficiently. We, however, believe that the discrepancy may also be due to finite-size effects: their correlation lengths at low temperatures increase with the lattice size (see Fig. 6 of Ref. 15) whereas in our calculation finite-size effects appear at larger correlation lengths (somewhat lower temperatures). This difference could be due to the different way of calculating the correlation function in the two calculations. Hence, it is possible that our results represented by the dashed line in Fig. 6 of Ref. 15, approximate better the infinite lattice. Using their values for $A_H = 0.32$ and $B_H \simeq 1$, we obtain $\hbar c \simeq 0.93 Ja_H$ which is somewhat lower than ours. If, on the other hand, we use the most recent form of Chakravarty, Halperin, and Nelson[16] who found $A_H = 0.467$ and $B_H = 0.94$, we find

$\hbar c \simeq 1.27 Ja_H$.

In Fig. 15 we plot the inverse correlation length versus T as observed by neutron scattering experiments.[3] The solid line corresponds to our Eq. (6.1) which fits both the nonlinear σ model and the spin-$\frac{1}{2}$ AF Heisenberg model using $J = 1270$ K, a value close to that reported by Raman scattering experiments.

VII. CONCLUSION

We have studied the quantum-mechanical nonlinear σ model in $2+1$ dimensions on a lattice. We have determined what should be the dependence of the coupling constant (spin stiffness) of the theory on the lattice spacing so that the results for the correlation length at any fixed physical temperature are independent of the cutoff in the continuum limit. At $T=0$ we found the critical point g_c that separates the disordered from the ordered phase of the σ model. As $T \to 0$ and at $g = g_c$, $\xi \simeq 0.8(\hbar c/k_B T)$. By calculating the model's renormalization group β function we rescale the calculated correlation lengths at various couplings and temperatures and find that they all collapse on the same curve $\xi/a_\sigma = f(T/T_\sigma)$. Even though the lattice spacing vanishes, dimensional transmutation occurs giving rise to a finite unit of length a_σ. Both parameters a_σ and the temperature scale $T_\sigma = \hbar c/a_\sigma$ (c is the unrenormalized spin-wave velocity which enters as a parameter in the partition function of σ model) of the theory cannot be determined within the σ model. We need to make contact with either the parameters of a microscopic model or with the experiment whose physics the σ model is assumed to describe.

The parameters a_σ and T_σ of the σ model can be related to the lattice spacing a_H and the AF coupling J of the spin-$\frac{1}{2}$ AF Heisenberg model. The numerical relationship between a_σ, T_σ, and a_H, J is obtained by fitting the $\xi(T) = f(T/T_\sigma)a_\sigma$ to the correlation length $\xi(T) = \xi_H(T/J)a_H$ obtained from the simulations of the spin-$\frac{1}{2}$ AF Heisenberg model.[5,6,15] As a consequence of the *assumption* that the two models are equivalent at low T we find that (a) the spin-$\frac{1}{2}$ AF Heisenberg model must order at $T=0$ and (b) the unrenormalized spin-wave velocity c, a parameter of the σ model, is obtained as $\hbar c = T_\sigma a_\sigma \simeq 1.04 Ja_H$. The value of $\hbar c$ obtained this way is not far from the value of the renormalized spin-wave velocity obtained from spin-wave theory of the spin-$\frac{1}{2}$ quantum Heisenberg antiferromagnet.

Having obtained a common curve which fits the spin-$\frac{1}{2}$ AF Heisenberg model and the nonlinear σ model we find that we need $J = 1270$ K to fit the neutron scattering data for the correlation length in the insulator La_2CuO_4. This value of J is close to that estimated by Raman scattering experiments.[17] Smaller values of J will bring our results closer to the data in that region but further away at higher T.
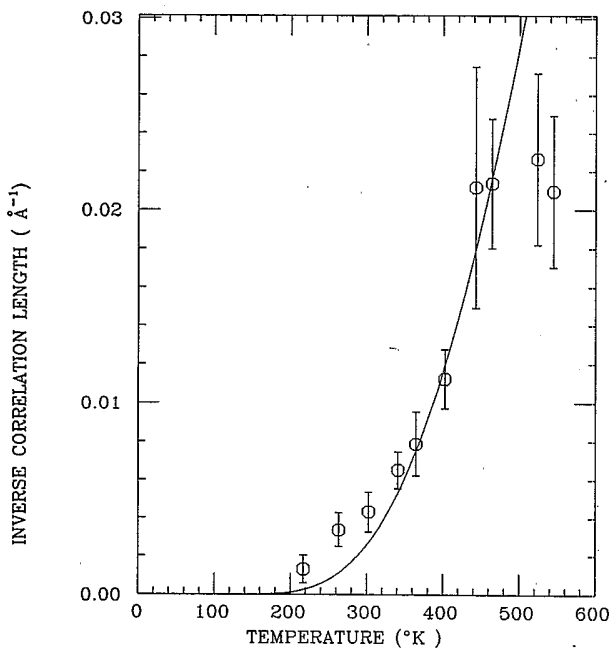

FIG. 15. Comparison with the neutron scattering data (Ref. 3) (open circles with error bars) taken on the insulator La_2CuO_4. The solid line represents our results for both the nonlinear σ model and the spin-$\frac{1}{2}$ AF Heisenberg model taking $J = 1270$ K a value close to that obtained by Raman scattering experiments (Ref. 17).

[1] J. G. Bednorz and K. A. Muller, Z. Phys. B **64**, 188 (1986); S. Uchida, H. Takagi, K. Katasawa, and S. Tanaka, Jpn. J. Appl. Phys. **26**, L1 (1987); C. W. Chu, P. H. Hor, R. L. Meng, L. Gao, Z. J. Huang, and Y. Q. Wang, Phys. Rev. Lett. **58**, 405 (1987); R. Cava, R. B. van Dover, B. Batlogg, and E. A. Rietmann, *ibid.* **58**, 408 (1987).

[2] D. Vaknin, S. K. Sinha, D. E. Moncton, D. C. Johnston, J. M. Newsam, C. R. Safinya, and H. E. King, Jr., Phys. Rev. Lett. **58**, 2802 (1987); G. Shirane, Y. Endoh, R. J. Birgeneau, M. A. Kastner, Y. Hidaka M. Oda, M. Suzuki, and T. Murakami, *ibid.* **59**, 1613 (1987); Y. Endoh *et al.*, Phys. Rev. B **37**, 7443 (1988).

[3] P. W. Anderson, G. Baskaran, Z. Zou, and T. Hsu, Phys. Rev. Lett. **58**, 2790 (1987).

[4] J. E. Hirsch, Phys. Rev. Lett. **54**, 1317 (1985); S. Kivelson, D. S. Rokhsar, and J. P. Sethna, Phys. Rev. B **35**, 8865 (1987); A. E. Ruckenstein, P. J. Hirschfeld, and J. Appel, *ibid.* **36**, 857 (1987); K. Huang and E. Manousakis, *ibid.* **36**, 8302 (1987); E. Kaxiras and E. Manousakis, *ibid.* **37**, 656 (1988).

[5] E. Manousakis and R. Salvador, Phys. Rev. Lett. **60**, 840 (1988).

[6] E. Manousakis and R. Salvador, Phys. Rev. B **39**, 575 (1989).

[7] F. D. M. Haldane, Phys. Lett. **93A**, 464 (1983); Phys. Rev. Lett. **50**, 1153 (1983).

[8] I. E. Dzyaloshinskii, A. M. Polyakov, and P. B. Wiegmann, Phys. Lett. A **127**, 112 (1988); P. B. Wiegmann, Phys. Rev. Lett. **60**, 821 (1988); A. M. Polyakov, Mod. Phys. Lett. A**3**, 325 (1988).

[9] T. Dombre and N. Read, Phys. Rev. B **38**, 7181 (1988); E. Fradkin and M. Stone, *ibid.* **38**, 7215 (1988); L. B. Ioffe and A. I. Larkin, Int. J. Mod. Phys. B **2**, 203 (1988); X.-G. Wen and A. Zee, Phys. Rev. Lett. **61**, 1025 (1988); F. D. M. Haldane, *ibid.* **61**, 1029 (1988).

[10] S. Chakravarty, B. I. Halperin, and D. Nelson, Phys. Rev. Lett. **60**, 1057 (1988).

[11] E. Manousakis and R. Salvador, Phys. Rev. Lett. **61**, 1310 (1989).

[12] M. Fukugita and Y. Oyanagi, Phys. Lett. **123B**, 71 (1983).

[13] S. Coleman and E. Weinberg, Phys. Rev. D **7**, 1888 (1973).

[14] T. Oguchi, Phys. Rev. **117**, 117 (1960).

[15] G. Gomez-Santos, J. D. Joannopoulos, and J. W. Negele, Phys. Rev. B **39**, 4435 (1989).

[16] S. Chakravarty, B. I. Halperin, and D. Nelson (unpublished).

[17] K. B. Lyons, P. A. Fleury, J. P. Remeika, and T. J. Nergan, Phys. Rev. B **37**, 2353 (1988).